Materials Science and Engineering A 417 (2006) 104–109

www.elsevier.com/locate/msea

Surface oxidation of NiTi shape memory alloy in a boiling aqueous solution containing hydrogen peroxide

C.L. Chu [a,*], C.Y. Chung [b], P.K. Chu [b]

[a] *Department of Materials Science and Engineering, Southeast University, Nanjing 210018, PR China*
[b] *Department of Physics and Materials Science, City University of Hong Kong, Hong Kong, PR China*

Received in revised form 4 October 2005; accepted 1 November 2005

Abstract

Oxidation behavior and surface characterizations of NiTi shape memory alloy (SMA) treated with a boiling H_2O_2 aqueous solution were investigated by scanning electron microscopy, X-ray diffraction, X-ray photoelectron spectroscopy, Fourier transform infrared spectroscopy and Raman spectroscopy. It is found that the low-temperature oxidation of NiTi SMA in H_2O_2 solution resulted in the formation of a titania scale enriched with Ti–OH groups. The titania scale is mainly composed of rutile and anatase, and is relatively depleted in Ni, which can improve the biocompatibility of NiTi SMA. Depth profiles of O, Ni and Ti show the titania scale possesses a smooth graded interface structure to NiTi substrate, which is in favor of high bonding strength of the titania scale with NiTi substrate. A different oxidation mechanism for NiTi SMA in H_2O_2 solution from that for NiTi SMA at high temperature air environment was proposed based on the experimental results.

Keywords: Shape memory alloy (SMA); NiTi; Oxidation; Surface structure

1. Introduction

NiTi shape memory alloy (SMA) has now attracted considerable attention in biomedical applications because of its unique properties such as shape memory effect, superelastic properties, good corrosion resistance and biocompatibility [1,2]. The surface structure is of interest for its effects on metal ion release, biocompatibility and corrosion of NiTi implants [3]. It is well known that the biocompatibility of NiTi implants depends on a native corrosion-resistant titanium oxide layer on the surface of NiTi SMA avoiding the allergic and toxic effects of nickel [4]. However, nickel either in metallic or in oxidized state is also detected on the surface of NiTi SMA, and its amount depends on the surface treatments [5,6].

The heat treatment in the environment containing oxygen will result in the oxidation of NiTi SMA and the formation of titanium oxide layer on its surface. Up to now, several oxidation treatments as well as the oxidation behaviors of NiTi SMA at high temperatures were reported [7–11]. Firstov et al. studied the surface oxidation of NiTi SMA subjected to heat treatment in air from 300 to 800 °C [8]. Xu et al. reported the isothermal oxidation behavior of NiTi SMA in pure oxygen over the temperature range 450–750 °C [9]. Chu et al. investigated the isothermal oxidation behavior of NiTi SMA in dry air from 550 to 1000 °C [10]. Chan et al. [11] studied the oxidation behavior of NiTi SMA at 400 °C in an oxygen pressure of 10^{-4} Torr or in air.

Recently, some studies indicate that titania films can be prepared by the low temperature oxidation of metallic Ti substrates in hydrogen peroxide solution [12–14]. However, few systematic studies have been reported to date on the low temperature oxidation behavior of NiTi SMA in hydrogen peroxide solution. The purpose of the present study was to systematically investigate the oxidation behavior and surface characterizations of NiTi SMA treated with a boiling aqueous solution containing hydrogen peroxide employing scanning electron microscopy (SEM), X-ray diffraction (XRD), X-ray photoelectron spectroscopy (XPS), Fourier transform infrared spectroscopy (FTIR) and Raman spectroscopy.

2. Experimental

A commercially available NiTi (50.8 at.% Ni) SMA plate for medical application with a martensite start temperature (M_s) of

* Corresponding author.
E-mail address: clchu@seu.edu.cn (C.L. Chu).

0921-5093/$ – see front matter © 2005 Elsevier B.V. All rights reserved.
doi:10.1016/j.msea.2005.11.010

−12.8 °C and an austenite finish temperature (A_f) of 33.4 °C was cut into small rectangular blocks ($10 \times 10 \times 1\,mm^3$). All samples were chemically polished to remove the original oxides on the surface for 10 min in Kroll's reagent: a mixture of 2 ml hydrofluoric acid (HF, 40%), 4 ml nitric acid (HNO_3, 40%) and 994 ml deionized water. The samples were subsequently ultrasonically washed in acetone for 10 min and in deionized water for 10 min. They were divided into two groups. The first group was used as control (denoted as the chemically polished one). The second group was further oxidized in a boiling aqueous solution containing 30%H_2O_2 for 2 h, and then ultrasonically rinsed with deionized water for 10 min (denoted as the H_2O_2-oxidized one).

Samples were XPS analyzed using a VG Scientific ESCALAB 5 spectrometer with monochromatic Al Kα (1486.6 eV) X-ray radiation. The operating vacuum conditions in the chamber were better than 10^{-8} mbar. Survey spectra in the range 0–1400 eV were recorded for each sample at a 50 eV constant pass energy, followed by higher resolution spectra over the Ti 2p, O 1s and Ni 2p ranges using a 20 eV pass energy. The high-resolution XPS spectra were used for assessment of the chemical state as well as for quantification. The experiments were repeated with at least three different samples. The XPS depth profiles were recorded using a rastered 3 keV Ar^+ ion beam at a rate of about 35 nm/min. XRD patterns of the samples were taken with an X-ray diffractometer (RAD IIA, Rigaku, Japan) operated with Cu Kα under 40 kV and 25 mA, equipped with a thin-film attachment on which the glancing angle was 1 °. FTIR spectra were recorded using FTIR spectrometry (Nicolet 800). Raman scattering spectra were recorded with a Renishaw system 2000 spectrometer, using the 514 nm line of Ar^+ for excitation. The light beam was focused to a spot of about 5 mm in size. The surface morphology of the samples was observed by Philips XL30 FEG SEM after the surfaces were coated with gold films. The accelerating voltage was 20 kV.

3. Results

Fig. 1 shows typical XPS survey spectra of the surfaces of NiTi SMAs. It could be found that the dominant surface elements are Ni and Ti for the chemically polished one and O for the H_2O_2-oxidized one, which suggests an oxide film formed on the H_2O_2-oxidized NiTi substrate. The surface amount of O on the chemically polished one is only about 7.9 at.%, while it is 58.4 at.% for the H_2O_2-oxidized one. Moreover, the surface content of Ni on the H_2O_2-oxidized one decreases remarkably from 47.5 at.% for the chemically polished one down to 6.7 at.%. The presence of C can be attributed to surface contamination by carbon-containing molecules absorbed from the environment. Fig. 2 shows SEM photographs of the surfaces of NiTi SMAs. Some submicron pores were observed on the chemically polished one, which may be due to the treatment with Kroll's reagent. After NiTi SMA was subsequently treated by H_2O_2 solution, the oxide film with some microcracks was present on NiTi substrates.

XPS depth profiles of NiTi SMAs are shown in Fig. 3. The amount of O on the surface of the freshly polished one decreases rapidly to zero after several minutes of sputtering. Depth profiles of O, Ni and Ti concentrations for the H_2O_2-oxidized one from the scale to the substrate exhibit different distributions (Fig. 3b). Both O and Ti have a peak close to the outmost surface, while Ni has a minimum value on the outmost surface of the oxide layer. After that, O has a step change, and then decreases gradually to zero. Ni has also a step change, and then passes through a gradual increase, and finally reaches its steady-state value of 58 at.%. Ti has a slow and slight increase, and then reaches a steady-state value of about 41 at%. The inconsistency of the steady-state values of Ni and Ti in the samples after the sputtering of Ar^+ ion beam with the chemical compositions of the untreated NiTi SMA (50.8 at% Ni) may be due to preferential sputtering of Ti [8]. The thickness of the oxide film on NiTi substrate oxidized with the boiling 30% H_2O_2 solution for 2 h is estimated in the described manner as 0.5 μm.

High resolution XPS collections of Ti binding energy regions were made as shown by Fig. 4. The XPS spectrum of the surface of the H_2O_2-oxidized one as received (Curve 1 in Fig. 4) exhibits two dominant peaks, namely Ti^{4+} (TiO_2) $2p_{3/2}$ at 459.3 eV and Ti^{4+} (TiO_2) $2p_{1/2}$ at 464.8 eV. Some remnants of combined Ti species could also be found by the presence of the small shoulders near 454.5 and 460.5 eV, which correspond to the binding energies of $Ti^{Ni–Ti}$ $2p_{3/2}$ and $2p_{1/2}$ spin states [15]. After argon ion sputtering, these two small shoulders near 454.5 and

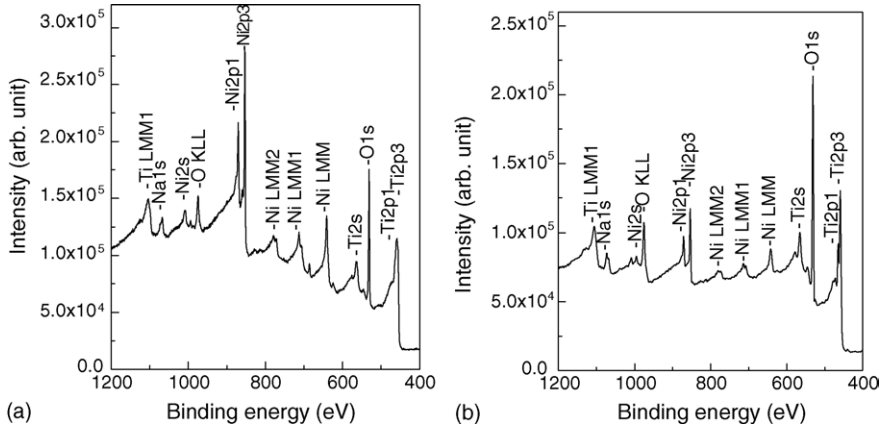

Fig. 1. XPS survey spectra of the surfaces of NiTi SMAs: (a) the chemically polished one; (b) the H_2O_2-oxidized one.

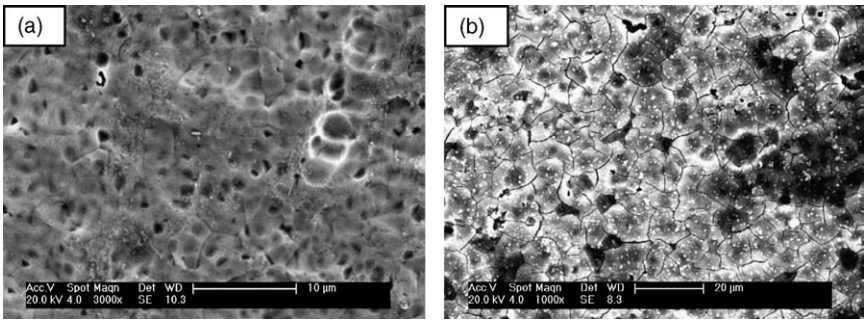

Fig. 2. SEM images of the surfaces of NiTi SMAs: (a) the chemically polished one; (b) the H_2O_2-oxidized one.

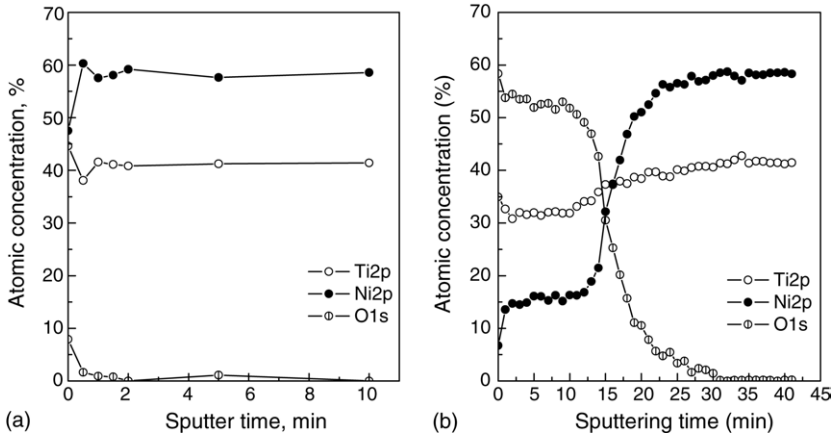

Fig. 3. XPS depth profiles of the surfaces of NiTi SMAs: (a) the chemically-polished one; (b) the H_2O_2-oxidized one.

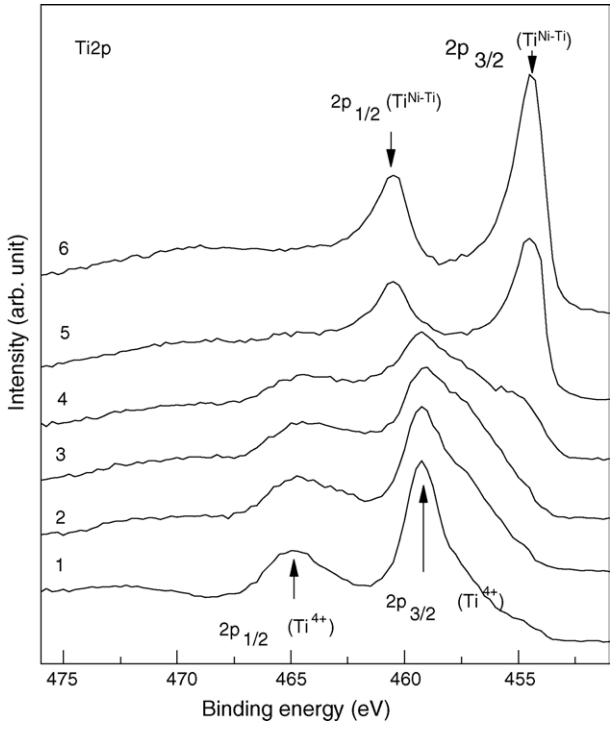

Fig. 4. Ti 2p XPS spectra of the surface of the H_2O_2-oxidized NiTi SMA after different time of sputtering: (1) as received; (2) 3 min; (3) 8 min; (4) 13 min; (5) 18 min; (6) 38 min.

460.5 eV change gradually into the dominant peaks, which indicates $Ti^{Ni–Ti}$ in intermetallic NiTi state, became the dominant Ti chemical state. After 38 min of sputtering, Ti was present only in intermetallic NiTi state.

Fig. 5 shows high resolution XPS collections of Ni binding energy regions. Ni 2p spectra of the surface of the H_2O_2-oxidized one mainly consist of two major peaks near 853.8 and 870.5 eV, which are assigned to $Ni^{Ni–Ti}$ $2p_{3/2}$ and $2p_{1/2}$ in intermetallic NiTi state [15]. It is necessary to point out that Ni oxide peak could not be found. After argon ion sputtering, $Ni^{Ni–Ti}$ 2p spectra exhibit a more evident satellite structure, which is separated from the main peaks by ~ 7 eV. O 1s spectra of the surface of the H_2O_2-oxidized one are shown in Fig. 6. The main peak has a binding energy of 530.8 eV and remains unchanged after argon ion sputtering, which can be assigned to oxygen present in metal oxides [5].

Raman spectra of the surfaces of the chemically polished one and the H_2O_2-oxidized one were recorded and are presented in Fig. 7. For both samples, the characteristic air bands are visible at low wave numbers up to $180 \pm 10\,cm^{-1}$ [16]. No additional bands are detected in the spectrum of the chemically-polished one. The existence of rutile and anatase on the surface of the H_2O_2-oxidized one is confirmed by the presence of bands at 220–280, 396 ± 10, 447 ± 10 and $514 \pm 10\,cm^{-1}$, respectively. The wide band at 220–280 cm^{-1} for typical rutile results from the second reflection or defects [17]. Raman measurements reported in the literature [17–19] indicate that the shift

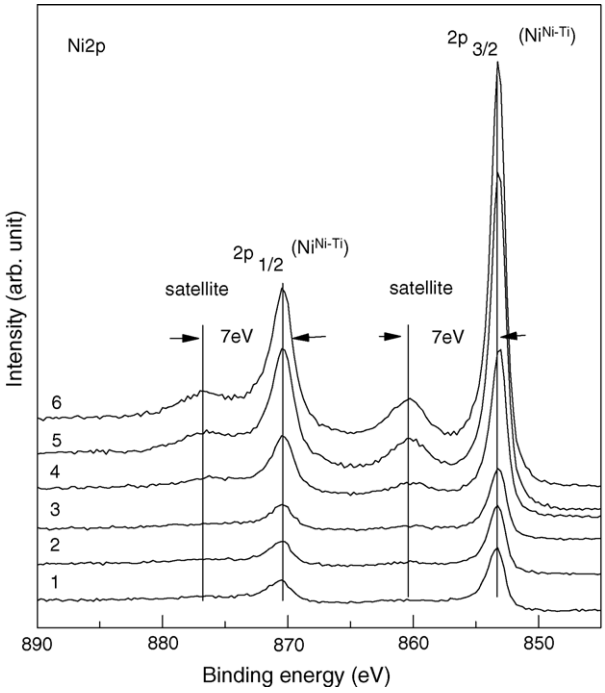

Fig. 5. Ni 2p XPS spectra of the surface of the H_2O_2-oxidized NiTi SMA after different time of sputtering: (1) as received; (2) 3 min; (3) 8 min; (4) 13 min; (5) 18 min; (6) 38 min.

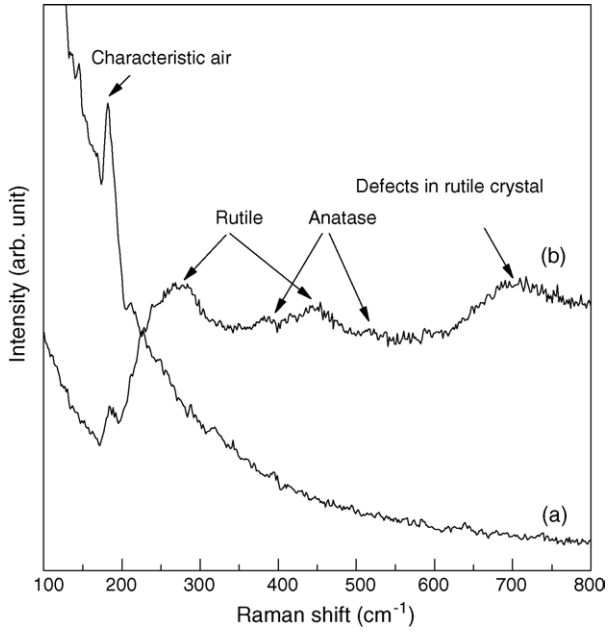

Fig. 7. Raman spectra of the surfaces of NiTi SMAs: (a) the chemically polished one; (b) the H_2O_2-oxidized one.

at 447 cm^{-1} is the E_g mode for rutile. Raman bands observed near 396 and 514 cm^{-1} correspond to the spectrum of anatase crystal [18,19]. The broadening of these bands suggests the relatively low crystalline of their respective Ti oxides. The band near 705 cm^{-1} in the spectrum (Fig. 7b) may come from the defects in Ti oxide crystal [17].

The characteristic parts of XRD patterns of the surfaces of NiTi SMAs are shown in Fig. 8. It can be found that except for intermetallic NiTi substrate phase, the broadening peaks associated with poorly crystallized rutile and anatase are present after the chemically polished one was oxidized with H_2O_2 solu-

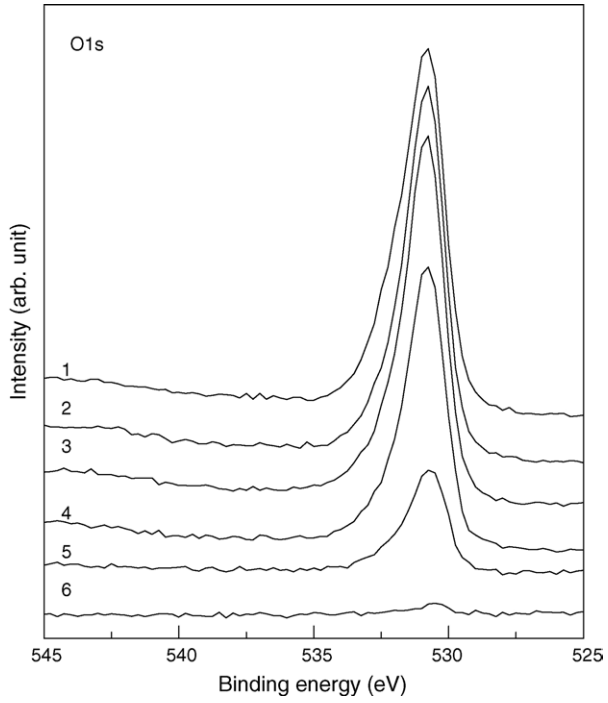

Fig. 6. O 1s XPS spectra of the surface of the H_2O_2-oxidized NiTi SMA after different time of sputtering: (1) as received; (2) 3 min; (3) 8 min; (4) 13 min; (5) 18 min; (6) 38 min.

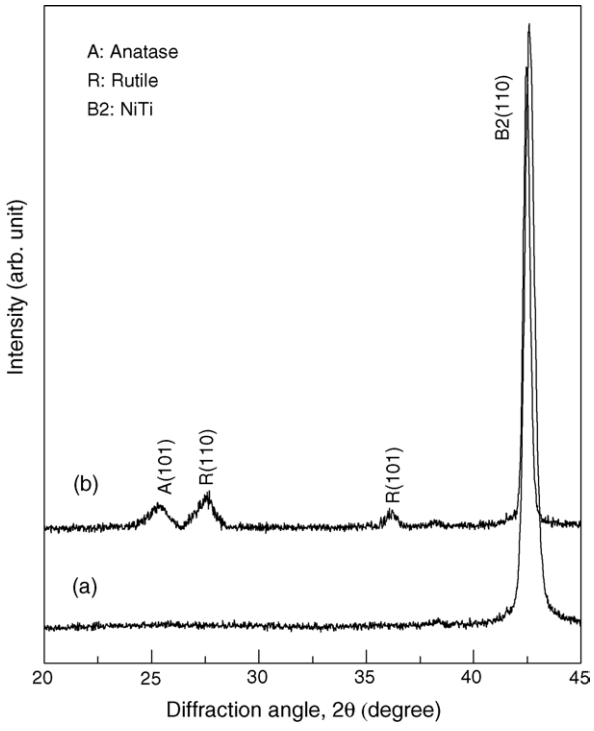

Fig. 8. XRD spectra of the surfaces of NiTi SMAs: (a) the chemically polished one; (b) the H_2O_2-oxidized one.

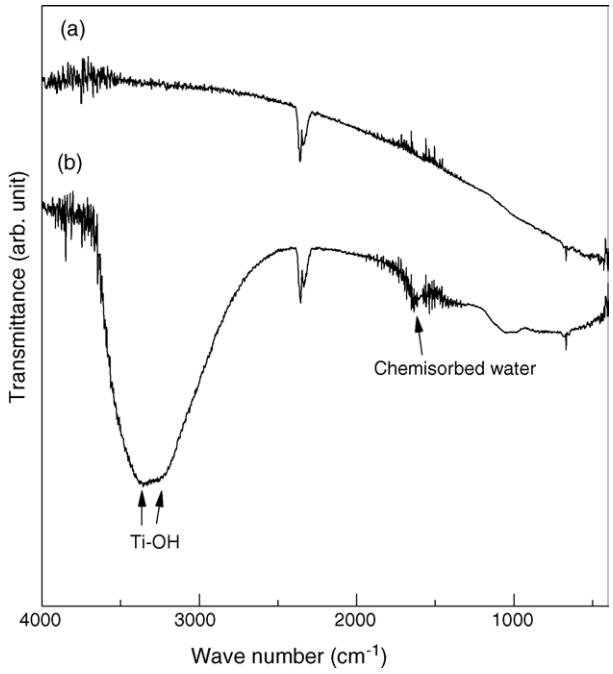

Fig. 9. FTIR spectra of the surfaces of NiTi SMAs: (a) the chemically polished one; (b) the H_2O_2-oxidized one.

tion. The results of FTIR spectroscopic measurements are shown in Fig. 9. In comparison with the spectrum of the surface of the chemically polished one, the one for the H_2O_2-oxidized one has some additional bands, e.g. two broad OH stretching bands at 3352 and 3233 cm^{-1} deriving from Ti–OH groups and the band at 1625 cm^{-1} corresponding to the bending mode of chemisorbed water [20,21].

4. Discussion

The results of XPS measurements for the chemically polished one indicate that the original oxides on the surface of NiTi substrate have been removed successfully, which can reduce the effect of original oxides on the oxidation behavior of NiTi SMA in H_2O_2 solution. After the chemically polished one was oxidized by H_2O_2 solution, XRD patterns display a consistent result as Raman spectra and XPS spectra that an oxide film consisted mainly of poorly crystallized rutile and anatase phases and depleted relatively in Ni was present on the surface of the sample. There was no Ni oxide or free Ni, thus the remnant Ni in the scale must be present as intermetallic NiTi phase, which has also been indicated by XPS analysis. The enrichment of Ti–OH groups on the surface of the H_2O_2-oxidized one is anticipated because NiTi substrate was oxidized under the aqueous conditions, and is in favor of the bioactivity of metal implants by inducing apatite deposition in simulated body fluid [22].

According to the experimental results, an oxidation mechanism of NiTi SMA in the boiling H_2O_2 solution is proposed as the following. In spite of the fact that NiTi SMA contains a large amount of Ni, there is no Ni oxide formed in the scale. This can reflect the difference in the oxygen affinity between Ti and Ni. As discussed in the literature [15], most metals react with oxygen at surface imperfections to form an oxide layer with a release of free energy. In this work, H_2O_2 was used as the oxidizing agent. The oxidizing reaction of NiTi SMA proceeds by the decomposition of H_2O_2 into oxygen. The heats of formation, ΔH_f, of TiO_2 and NiO are approximatively estimated according to the following reactions [23],

$$Ti(s) + O_2(g) \rightarrow TiO_2(s) \qquad \Delta H_f = -956\,kJ\,mol^{-1} \quad (1)$$

$$Ni(s) + 1/2O_2(g) \rightarrow NiO(s) \qquad \Delta H_f = -241\,kJ\,mol^{-1} \quad (2)$$

The large disparity between the above values that the formation enthalpy of TiO_2 is almost four times of the one for NiO may reflect the stronger affinity of Ti than that of Ni for oxygen chemisorption. Therefore, Ti on the outermost surface of NiTi SMA in H_2O_2 solution is oxidized firstly by oxygen derived from the decomposition of H_2O_2 to form TiO_2 while Ni remains unchanged. Ni atoms can be removed from Ni–Ti bond due to H_2O_2-etching, leave the surface and are released into the aqueous solution during boiling. The release of Ni atoms from the surface of NiTi SMA into the boiling water has been found by Shabalovskaya et al. with the aid of inductively coupled plasma analysis (ICPA) [5]. Ti bound in oxide is more stable and is not released into the aqueous solution. The release of Ni atoms into the aqueous solution leads to the presence of vacancies at the interface between the oxide scale and NiTi substrate, which can promote the further reaction of oxygen with Ti atoms. The predominant phase TiO_2 in the scale has a larger unit cell volume (0.062 nm^3 for rutile) than austenitic NiTi substrate (0.027 nm^3) [15]. The larger TiO_2 crystal structure is accommodated by O migration towards the NiTi substrate and Ni migration towards the surface. As the oxidation progresses, O atoms diffuse inward while Ni atoms diffuse outward through the scale. Consequently, the oxide scales composed mainly of TiO_2 and depleted relatively in Ni form on NiTi substrate. It is obvious that the low-temperature oxidation of NiTi SMA in H_2O_2 solution is dominated by an inward growth of the oxide and the oxidation rate is mainly controlled by the diffusion rate of O and Ni atoms in the oxide scale. As the scale grows, the oxidation rate will decrease due to the longer diffusion path for O and Ni atoms and high stress will be built up in the scale due to the volume difference between the oxide and NiTi substrate. The latter can lead to the formation of microcracks in the oxide scale as shown by Fig. 2b.

This oxidation mechanism for NiTi SMA in H_2O_2 solution is different from that for NiTi SMA at high temperature air environment proposed by Chu et al. [10]. According to the latter, an outward growth of titanium oxide due to the outward diffusion of Ti from metal at high temperature will lead to the formation of $TiNi_3$ phase in a Ni-rich layer between the scale and NiTi substrate, which has also been confirmed by Chu et al. [10]. However, this Ni-rich layer was not found by our studies. In the present work, the boiling aqueous solution can promote the release of Ni atoms from NiTi surface. As supported by the depth profiles of O, Ni and Ti concentrations for the H_2O_2-oxidized one (Fig. 3b), the inward growth of the oxide with the outward

diffusion of Ni atoms from metal to the solution can result in the presence of a graded interface structure between the scale and NiTi substrate, which is in favor of high bonding strength of the scale with NiTi substrate.

Surface oxidation in H_2O_2 solution can lead to the formation of titania film and remove Ni synchronously from NiTi surface into the aqueous solution, which can significantly reduce the release amount of Ni ions and improve the biocompatibility of NiTi implants in the physiological environment. The remnant of Ni present as NiTi phase in titania film may be due to the insufficient oxidation reaction of NiTi SMA and the incomplete removal of Ni into the aqueous solution under the given conditions. The optimized oxidation techniques as well as the effects of surface oxidation in H_2O_2 solution on the biocompatibility and corrosion resistance of NiTi SMA are being pursued and will be reported in due course.

5. Conclusions

The chemically polished NiTi SMA was oxidized with a boiling hydrogen peroxide solution, and then characterized systematically by SEM, XRD, XPS, FTIR and Raman spectroscopy. The study leads to the following important conclusions.

(1) Surface oxidation of NiTi SMA in the boiling hydrogen peroxide solution resulted in the formation of a titania scale enriched with Ti-OH groups. The titania scale was mainly composed of rutile and anatase phases, and was relatively depleted in Ni, which can improve the biocompatibility of NiTi SMA.
(2) Depth profiles of O, Ni and Ti show the titania scale on the H_2O_2-oxidized NiTi SMA possesses a smooth graded interface structure to NiTi substrate, which is in favor of high bonding strength of the titania scale with NiTi substrate.
(3) The low-temperature oxidation of NiTi SMA in H_2O_2 solution is dominated by an inward growth of the oxide and the oxidation rate is mainly controlled by the diffusion process of O inward migration and Ni outward migration through the oxide scale, which are different from those for NiTi SMA at high temperature air environment.

Acknowledgements

The work described in this paper was supported by four grants from the Natural Science Foundation of Jiangsu Province under the contract BK2003062, the Research Grants Council of the Hong Kong Special Administrative Region (Project no. 8730021), the Teaching and Research Award Program for Outstanding Young Teachers of Southeast University (Project No.: 4012001007), National Natural Science Foundation of China (Project no.: 50501007).

References

[1] T. Duerig, A. Pelton, D. Stockel, Mater. Sci. Eng. A273–A275 (1999) 149.
[2] K. Otsuka, C.M. Wayman, Shape Memory Materials, Cambridge University Press, Cambridge, 1998.
[3] B.D. Ratner, A.S. Hoffman, F.J. Schoen, J.E. Lemons, Biomaterials Science, Academic Press, London, 1996.
[4] D.J. Wever, A.G. Veldhuizen, J. de Vries, H.J. Busscher, D.R.A. Uges, J.R. van Horn, Biomaterials 19 (1998) 761.
[5] S.A. Shabalovskaya, J.W. Anderegg, J. Vac. Sci. Technol. A13 (5) (1995) 2624.
[6] P. Filip, J. Lausmaa, J. Musialek, K. Mazanec, Biomaterials 22 (2001) 2131.
[7] D.A. Armitage, D.M. Grant, Mater. Sci. Eng. A349 (2003) 89.
[8] G.S. Firstov, R.G. Vitchev, H. Kumar, B. Blanpain, J.V. Humbeeck, Biomaterials 23 (2002) 4863.
[9] C.H. Xu, X.Q. Ma, S.Q. Shi, C.H. Woo, Mater. Sci. Eng. A371 (2004) 45.
[10] C.L. Chu, S.K. Wu, Y.C. Yen, Mater. Sci. Eng. A216 (1996) 193.
[11] C.M. Chan, S. Trigwell, T. Duerig, Surf. Interface Anal. 15 (1990) 349.
[12] S. Takemoto, T. Yamamoto, K. Tsuru, S. Hayakawa, A. Osaka, S. Takashima, Biomaterials 25 (2004) 3485.
[13] J. Wu, S. Hayakawa, K. Tsuru, A. Osaka, Scr. Mater. 46 (2002) 101.
[14] X.X. Wang, S. Hayakawa, K. Tsuru, A. Osaka, J. Biomed. Mater. Res. 52 (2000) 171.
[15] S.M. Green, D.M. Grant, J.V. Wood, Mater. Sci. Eng. A224 (1997) 21.
[16] A.P. Pino, P. Serra, J.L. Morenza, Thin Solid Films 415 (2002) 201.
[17] X. Li, T. Kobayashi, T. Sekine, Solid State Commun. 130 (2004) 79.
[18] S.M. Oh, T. Ishigaki, Thin Solid Films 457 (2004) 186.
[19] T.D. Robert, L.D. Laude, V.M. Geskin, R. Lazzaroni, R. Gouttebaron, Thin Solid Films 440 (2003) 268.
[20] S. Music, M. Gotic, M. Ivanda, S. Popovic, A. Turkovic, R. Trojko, A. Sekulic, K. Furic, Mater. Sci. Eng. B47 (1997) 33.
[21] V.A. Skryshevskyy, Th. J. Dittrich, J. Rappich, Phys. Stat. Solidi A201 (1) (2004) 157.
[22] P. Li, C. Ohtsuki, T. Kokubo, K. Nakanishi, N. Soga, K. DeGroot, J. Biomed. Mater. Res. 28 (1994) 7.
[23] R.C. Weast, M.J. Astle, CRC Handbook of Chemistry and Physics, CRC Press, Boca Raton, Florida, 1982.